Journal of Theoretical Biology 373 (2015) 73–81

Contents lists available at ScienceDirect

Journal of Theoretical Biology

journal homepage: www.elsevier.com/locate/yjtbi

Retinogenesis: Stochasticity and the competency model

A. Barton [a], A.J. Fendrik [a,b,*]

[a] Instituto de Ciencias, Universidad Nacional de General Sarmiento, J.M. Gutierrez 1150, (1613) Los Polvorines, Buenos Aires, Argentina
[b] Consejo Nacional de Investigaciones Científicas y Técnicas, Buenos Aires, Argentina

HIGHLIGHTS

- We propose a stochastic model of retinogenesis for vertebrates.
- It is consistent with experimental data from rat retinogenesis.
- The process is controlled by a single factor that is stochastically inherited by daughter cells.
- This single factor not only controls the differentiation but also defines the competency to produce each phenotype of retinal cells.
- The model describes the complete development of the retina, the two phases and the intermediate stage between them.

ARTICLE INFO

Article history:
Received 1 October 2014
Received in revised form
9 March 2015
Accepted 12 March 2015
Available online 20 March 2015

Keywords:
Retinal progenitor cells
Stochastic development
Asymmetric divisions

ABSTRACT

The vertebrate retina is made up of seven principal cell types. These seven retinal cell types arise from multipotent retinal progenitor cells (RPCs). The competency model was proposed suggesting that RPCs undergo a series of irreversible transitions between competency states, in each of which the RPCs are competent to generate a different subset of cell types, but not retinal cells generated at previous moments. In this work, we generalize the stochastic model of neurogenesis of Barton et al. (2014), assuming that the same factor that regulates the differentiation, regulates the competency. The model reproduces the timing of production of different retinal cell types in rats such as it was experimentally measured. The results show that the evolution of the competency during retinogenesis could be explained by a single factor. Its evolution during the cell cycle and the stochastic inheritance in cell divisions determine the sequence and the overlap of production of different retinal cell types during development.

1. Introduction

The central nervous system (CNS) is composed of a large variety of neuronal and glial cell types derived from a population of stem/progenitor cells. The number and proportion of each cell type is critical for its correct operation, so that a key issue is to understand how the population of stem/progenitor cells generates a progeny of different cell types and how the progeny of each of the lineages reflects the repertoire of neural diversity. The vertebrate retina, which is part of the CNS, is a well characterized and experimentally accessible system for studying these issues. It is made up of seven principal cell types: six kinds of neurons (retinal ganglion cells, horizontal cells, bipolar cells, amacrine, cone photoreceptors and rod photoreceptors) and a type of glia (Müller glial cells). These retinal cell types arise from multipotent retinal cells (RPCs) in a chronological order (Livesey and Cepko, 2001): ganglion cells, horizontal cells, cone photoreceptors, amacrine cells, rods photoreceptors, bipolar cells and Müller (glial) cells, with some degree of overlap between the moments of production of the various cell types.

Furthermore, the lineages generated at clonal density are, as a population, undistinguishable in size and composition from the clones generated from retina explants of the same age (Cayouette et al., 2003). In addition, early RPCs produce cells with early fates when transplanted to delayed environments and vice versa (Belliveau and Cepko, 1999; Belliveau et al., 2000). All this suggests that the succession of competency states is an intrinsic process, that is independent of environmental cues. In an extrinsic process, all the cells would have the same competence at any time and environmental cues would direct the fate of their progeny (Cepko, 2014).

Based on these results, the competency model was proposed, suggesting that each RPC lineage undergoes a fixed series of changes in competency states, in each of which, at a given moment, the RPCs are competent to generate a specific subset of retinal cell types, different from the subset generated before (Cepko et al., 1996; Livesey and Cepko, 2001).

* Corresponding author at: Instituto de Ciencias, Universidad Nacional de General Sarmiento, J.M. Gutierrez 1150, (1613) Los Polvorines, Buenos Aires, Argentina.
E-mail addresses: alebarton@gmail.com (A. Barton), afendrik@ungs.edu.ar (A.J. Fendrik).

http://dx.doi.org/10.1016/j.jtbi.2015.03.015
0022-5193/

As in the case of generation of neuroblasts in *Drosophila* CNS, the competency states could occur by the expression of different transcription factors (Livesey and Cepko, 2001); although, unlike vertebrates, in *Drosophila* the succession of competency states occurs without overlap. At first, the above mentioned overlap could be due to heterogeneity in the competency states of individual RPCs at early stages of development. Thus, the composition of cell types of the adult retina would result different sequences of competency states operating in parallel in a deterministic way. In fact, this possibility is consistent with the heterogeneity observed in the transcriptomes of individual RPCs (Trimarchi et al., 2008).

Another competency model assumes that there are different types of RPCs established early in retinal development, each of which displays its lineage program previously specified (Cayouette et al., 2003; Cepko, 2014). According to this model, the distribution of cell types in the retina comes from the confluence of different patterns of lineage. This vision is conceptually similar to ventral nerve cord development in *Drosophila*, where positional values along the embryonic axes (anterior–posterior and dorsal–ventral), establish the fate of neuroblasts along the nerve cord. In turn, each neuroblast originates a clone composed of a given subset of cell types. In each mitosis another neuroblast and a terminally dividing cell (ganglion mother cell, GMC) are originated. As the neuroblasts undergo a succession of competency states, a single neuroblast originates GMCs of different types, each with its own progeny cell types (Li et al., 2013). In vertebrates, this model has received experimental basis from the identification of cells that produce two postmitotic daughter cells, similarly to the terminally dividing cells characterized in *Drosophila* (Cepko, 2014).

A remarkable feature of the clones derived from RPCs, marked with different techniques, is its diversity, both in size and composition (Turner and Cepko, 1987; Turner et al., 1999). There are two possible interpretations for the observed variability: (1) it reflects a diversity of individually predictable lineages (and asynchronous to each other in their competency state); (2) it is the result of stochastic decisions within a population of identical RPCs (Cayouette et al., 2003; Cayouette et al., 2006). The two models outlined so here does not assume stochasticity in the competency evolution. For example, in the original competency model (Cepko et al., 1996), diversity may be because an RPC does not produce postmitotic cell daughters in every competency state. The production could be regulated by mechanisms that are independent of the competency states.

To distinguish between these two alternatives, Gomes et al. (2011) used a videomicroscopy method to track individual images of perinatal rat RPCs (E20, embryonic day 20). Using this technique, RPCs are cultured at clonal density and the development of generated lineage is recorded by video microscopy (long-term time-lapse microscopy). RPCs can be distinguished from differentiated cells by morphological criteria, while the various differentiated cell types are distinguished by immunostaining of specific markers of each cell type at the end of the recording. Thus, it is possible to follow the order of cellular birth within individual clones and to do a statistical analysis of the division modes and choices of fate. The results show constant ratios for the occurrence of the different modes of division (RPC/RPC, RPC/differentiated cell, differentiated cell/differentiated cell) within lineages.

From this result, Gomes et al. (2011) propose a model in which the RPCs are divided with constant probabilities obtained from the mentioned ratios. In this way, they can reproduce the size distribution of clones observed experimentally. With these results, Gomes et al. (2011) suggest that, at least in vitro, from E20, the division modes of the RPCs are stochastic with more or less fixed probabilities.

Regarding the birth order of the different cell types, birth dating experiments in vivo show a chronological order (Rapaport et al., 2004) which is reproduced in cultures at clonal density (Cayouette et al., 2003). This could suggest that the timing of retinal production cell is the result of a determined succession of transitions among the competency states of individual RPCs.

However, in these studies birth order is analysed in terms of the total population and not in term of the lineages generated from individual RPCs. To address this point, Gomes et al. (2011) observe lineages formed by two or more cells, and they determine the frequency of production for different types of cells in the same lineage production. They observe some violations in birth order predicted by in vivo studies.

In addition, the comparison of pairs of cells originating from two successive divisions with those obtained in a stochastic model with fixed probabilities of production for each type of cells shows that the proportion of cell types may be reproduced by a stochastic mechanism of production with some probabilities for each cell type. These observations led these authors to suggest that in the vertebrate retina, the order of production of cell types is not strictly encoded in individual lineages.

This set of observations led to a probabilistic vision of retinogenesis, according to which each RPC, takes a series of stochastic decisions related to the mode of division and the originated cell types.

However, a question that arises from these results is whether the homoeostatic proportions of the different cell types of the adult retina can arise from modes of division and stochastic fate choices. To answer this question, He et al. (2012) have developed a method to trace lineages in zebrafish, using a variation of the MAZe (mosaic analysis in zebrafish) strategy (Collins et al., 2010), which allows marking individual RPCs and their progeny by fluorescence and to trace the evolution of the lineage in vivo by confocal microscopy 4D. Their results have revealed variations in the size of the clones that are reproduced by a model of fixed probabilities for modes of division. Regarding cell fates, the combination of different phenotypic ratios obtained from multiple lineages reproduces the fractions of cell type observed in retinal histogenesis in previous experiments of birth dating in zebrafish (Jusuf et al., 2011). Moreover, at clonal level, those authors note that in the mitosis, each cell type may have as a sister cell of more than one phenotype. That is, the analysis of retinogenesis of zebrafish in vivo reveals that the overlap in the generation of different cell types observed in birth dating experiments may be the result of stochastic processes at the level of individual clones that produce an adult retina with a distribution of invariant cell types at population level.

In summary, this set of observations in rat and zebrafish is consistent with stochastic processes on the choice of cell fate and division modes in vertebrate retinogenesis. It is currently being discussed the role of stochasticity in developmental lineage programs (Slater et al., 2009; Barton et al., 2014; Gomes et al., 2011; He et al., 2012) as well as the election of fate for stem cells of adult tissues (Klein and Simons, 2011). In a previous work (Barton et al., 2014), we study the potential role of asymmetric inheritance in the mitosis as a source of stochasticity for neurogenesis in mouse neocortex. In that work, we assume that neurogenesis is controlled by a concentration of a single neurogenic factor x which it is stochastically inherited between daughter cells after mitosis.

In that way, we were able to reproduce the evolution of the fractions of progenitor cells (P) and differentiated neurons (Q) during neurogenesis observed experimentally.

As in cortical neurogenesis, in retinogenesis the asymmetric division also has a role in the phenotypic diversity (Cayouette and Raff, 2003).

Moreover, Rapaport et al. (2004) show that retinogenesis can be divided into two phases with a transitional intermediate regime. During phase 1 are mostly generated ganglion cells, horizontal cells and cones cells while in phase 2 rod cells, bipolar cells and Müller glial cells are mainly produced. Between two phases, generation of amacrine cells occurs and it partially overlaps with both phases.

In this paper, we perform a change in the model of Barton et al. (2014): assuming that the same variable x regulates the differentiation and the competency (which defines the phenotype of the differentiated cells). We reproduce the experimental results on retinal cell production obtained by Rapaport et al. (2004). The results show that the evolution of the competency during retinogenesis can be explained by the evolution of a master factor that sets different thresholds of competency. Its evolution and the stochastic inheritance determine the sequence and the overlap in the generation of different cell types during retinal development. To our knowledge, this is the first quantitative model describing in a unified way the retinal development.

The paper is organized as follows. In Section 2 we briefly describe the original model of Barton et al. (2014). In Section 3 we establish the relationship between cell cycle and development days and we indicate the changes made to the original model. In Section 4 we show how the model reproduces global aspects of developing retina (total fraction of differentiated cells as development proceeds, division mode probabilities, P and Q). In Section 5, we introduce the parameters that define the competency and we adjust them to reproduce the overall fraction of each phenotype present at the end of retinal development. From this setting, we show the daily production for each cell type predicted by the model and we compare them with the experimentally measured. Finally, Section 6 is devoted to discuss the results.

2. The model

Our model of retinogenesis is based on the model of neurogenesis shown in Barton et al. (2014), in which we have made some changes. In order to facilitate the reading of this paper, we describe the original model and then we indicate the modifications we have introduced.

We assume that cellular concentration of a certain molecule x controls the neurogenesis process. Initially, the first progenitor cell has a concentration $x = x_o$ (which we take as a unit).

The concentrations of x, inherited by both cells after the first division (namely $x_1^1(t=0)$ and $x_2^1(t=0)$) are not independent since they are related by the following link:

$$x_1^1(t=0)+x_2^1(t=0)=2x_o. \tag{1}$$

Here the superscript indicates the generation and the subscript identifies the individual sibling cell. The constrain to Eq. (1) states that if one of the sister cells inherits a high concentration of x, the other will inherit a low concentration. We assume that the inherited concentration of one sister cell, say $x_1^1(t=0)$, is determined by some probability distribution $P(x)$, whose most probable value is x_o (that is where $P(x)$ is maximum). More precisely, the probability that the concentration inherited by a daughter cell falls between x and $x+dx$ is $P(x)\,dx$. Correspondingly, the concentration inherited by the other sister ($x_2^1(t=0)$) can be readily derived through Eq. (1). If the inherited concentration ($x_1^1(t=0)$ or $x_2^1(t=0)$) is less than or equal to certain critical value x^*, the daughter cell will remain in a proliferative state, otherwise the cell leaves the cycle as a neuron or glial cell. For cells remaining in a proliferative state, we assume that the synthesis of x between cell divisions (cycles) obeys the following equation:

$$\frac{dx}{dt}=\beta(N_c)-\nu\frac{x}{k+x}, \tag{2}$$

where $\beta(N_c)$ is the rate of synthesis of x which depend on the cell cycle number (N_c) and we assume a Michaelis–Menten degradation process of parameters ν and k. Hence, if $x_1^1(t=0)\le x^*$ (and/or $x_2^1(t=0)\le x^*$), to determine the concentration of x just before the second division, we integrate Eq. (2) starting from $x_1^1(t=0)$ (and/or $x_2^1(t=0)$) to obtain $x_1^1(t=T_1)$ (and/or $x_2^1(t=T_1)$). Here T_1 is the time between the first and the second cell division, i.e. the duration of the cell cycle. For the second cellular division, the progenitor cell has a concentration $x_1^1(t=T_1)$ (and/or $x_2^1(t=T_1)$). Hence the daughter cells will have concentrations linked by

$$x_1^2(t=0)+x_2^2(t=0)=2x_1^1(t=T_1); \tag{3}$$

and/or

$$x_3^2(t=0)+x_4^2(t=0)=2x_2^1(t=T_1). \tag{4}$$

Now, the probability of inheritance for $x_1^2(t=0)$ (and/or $x_3^2(t=0)$) will be given by $P'(x)$ similar to $P(x)$ but will have its maximum value at $x_1^1(t=T_1)$ (or $x_2^1(t=T_1)$).

The value of $x_2^2(t=0)$ (and/or $x_4^2(t=0)$) is determined by the link Eq. (3) (and/or Eq. (4)). Each time the concentration of x is less than or equal to the critical value x^*, we repeat this procedure on each of subsequent cell divisions (see Fig. 1). That is, if the cell k of generation j inherits $x_k^j(t=0)\le x^*$, it remains in a proliferative state. Then we evolve x_k^j, from $t=0$ to $t=T_j$ through Eq. (2). When

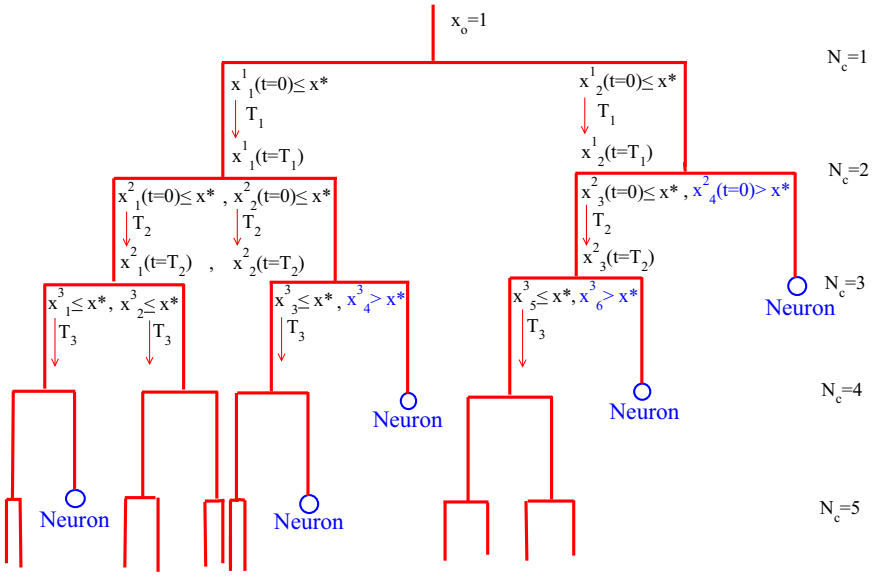

Fig. 1. Rules for the generation of cell lineage trees.

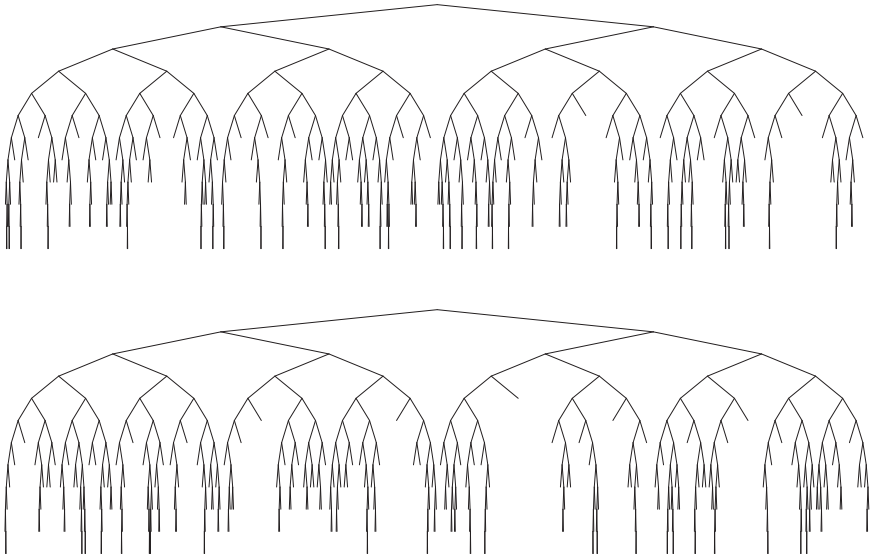

Fig. 2. Two realizations for cell lineage trees according to the rules explained in the text.

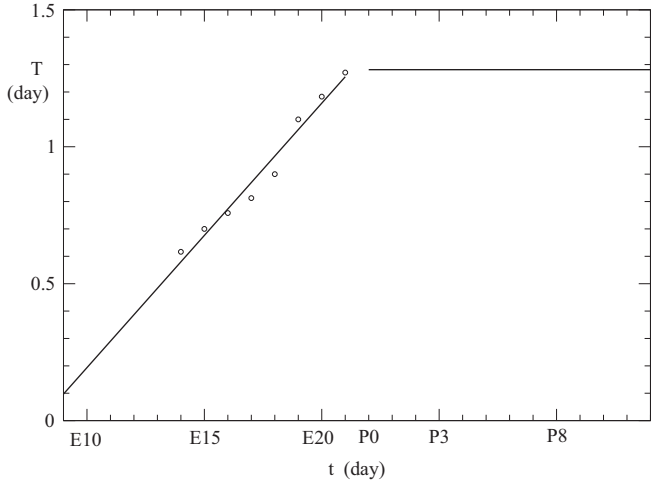

Fig. 3. Cell cycle length vs. age. The circles correspond to experimental values taken from Alexiades and Cepko (1996). These values were fitted by a linear function until the E21. After, the cell cycle length is taken as a constant.

mitosis occurs, the concentrations of the daughter cells will be related by

$$x_i^{j+1}(t=0)+x_{i+1}^{j+1}(t=0)=2x_k^j(t=T_j). \tag{5}$$

The concentration $x_i^{j+1}(t=0)$ is determined through the probability distribution $P(x)$ whose maximum is at $x_k^j(t=T_j)$. The second concentration $x_{i+1}^{j+1}(t=0)$ is determined by Eq. (5).

Thus we obtain similar lineage trees to those shown in Fig. 2.

We used as probability distribution $P(x)$, a Gaussian with a width σ proportional to the most probable value, that is $\sigma=(a/2)x_o$. In that way, we avoid possible non-biological values for x (i.e. $x<0$).

Let us remember that the distribution $P(x)$ is updated before each cell division so that the most probable value (here denoted as x_o) becomes the concentration of progenitor cell. In all cases we set the value of $a=0.2$, which leads to fluctuations in the inherited x from about 10% of the most probable value. All results are the average of 3000 realizations.

3. Rat retinogenesis

There are a lot of experimental data relating to retinal development in different species. For example, rat (Rapaport et al., 2004), monkey (LaVail et al., 1991) and wallaby (Harman and Beazley, 1989). Retinogenesis in each case presents several similarities as well also particular characteristics. Among conserved features we can mention the sequence in which the various types of cells are generated and the existence of two phases. Our idea is to reproduce these preserved features more than the characteristic details shown by each particular species. Our model presupposes knowledge on the behavior of the cell cycle length T as a function of the age, not only for the integration of Eq. (2) but also to transform the cell production per cycle to daily output. The only work we have found where experimental data on T are reported, it is precisely in rat (Alexiades and Cepko, 1996). That is why we apply the model to rat retinogenesis.

It is known that retinal development occurs between the ninth day of embryonic development (E9) and the 12th postnatal day (P12). Since gestation is approximately 22 days, retinal development occurs in 26 days.

It is also known that during this process the cell cycle length T is variable at the embryonic stage. In Fig. 3A of Alexiades and Cepko (1996) can be seen cell cycle length as a function of development time (age, we will denoted as t) determined by two different methods. Both methods lead to the same result (linear growth) in the embryonic stage. At the postnatal stage, while a method suggests that linear growth continues, the other seems to show that cell cycle length is constant. Other studies *in vitro* (Gomes et al., 2011) have found out that besides fluctuations, cell cycle length at the postnatal stage is constant, but its value is greater than that reported in Alexiades and Cepko (1996). Then we assume that cell cycle length increases linearly until birthday and from there it remains constant. From the data shown in Fig. 3A of Alexiades and Cepko (1996), we obtain the best linear fit shown in Fig. 3. Hence

$$T(t)=\begin{cases} a\times t+b & \text{if } 9 \text{ day} \le t \le 21 \text{ day}, \\ c & \text{if } 22 \text{ day } (P0) < t; \end{cases} \tag{6}$$

where $a=0.09654$, $b=-0.7718$ day and $c=1.2817$ day.

Unfortunately, since the experimental data are available from E14 day, we must extrapolate Eq. (6) to E9 day. From this fit, we obtain the cell cycle length T depending on the cycle number N_c and the development time t depending on the cycle number

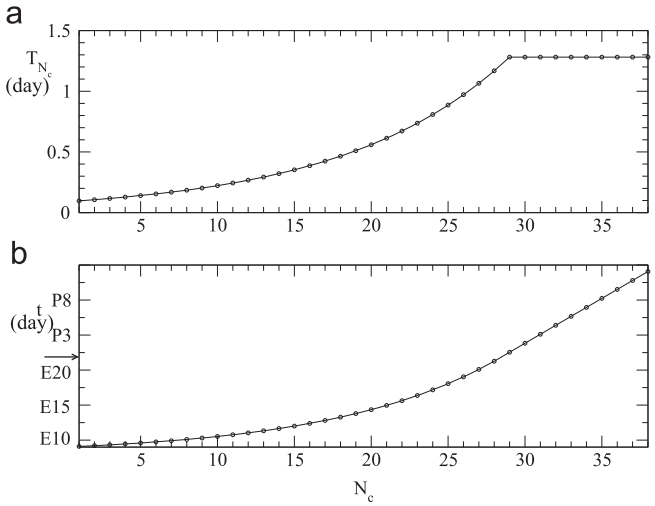

Fig. 4. (a) Cell cycle length, T_{N_c} vs. cell cycle number, N_c. (b) Age vs. cell cycle number, N_c. The arrow in the vertical axis indicates the birth day. Both graphics are obtained from Fig. 3 following the procedure explained in the text.

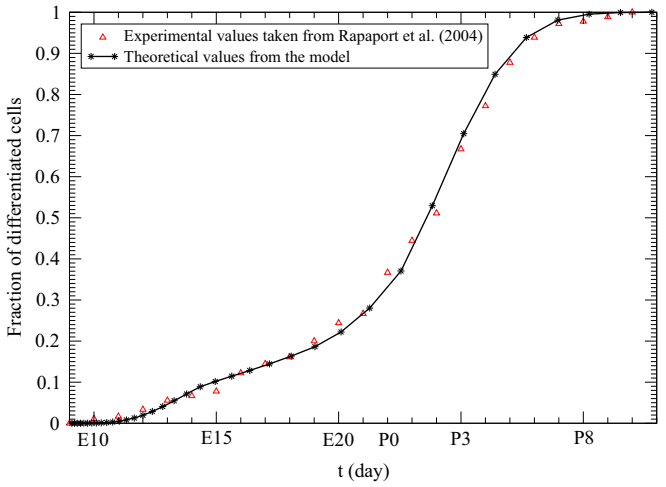

Fig. 5. Fraction of differentiated cells vs. age. The triangles correspond to experimental values taken from Rapaport et al. (2004). The stars correspond to the results following the present model of retinogenesis.

respectively as follows. The first cellular cycle for retinogenesis corresponds to 9 days. So following Eq. (6), we know T_1, that is cellular cycle length of the first cycle. Inserting (9 day $+T_1$) in Eq. (6), we obtain the T_2. To obtain T_3, we insert (9 day$+T_1+T_2$) in Eq. (6), etc. That is

$$T_{N_c} = \begin{cases} a \times \left(9\ \text{day} + \sum_{i=1}^{i=(N_c-1)} T_i\right) + b & \text{if } 1\ \text{day} \le N_c \le 29\ \text{day}, \\ c & \text{if } 30\ \text{day} \le N_c. \end{cases} \quad (7)$$

On the other hand, the age t is

$$t = 9\ \text{day} + \sum_{i=1}^{i=N_c} T_i; \quad (8)$$

when N_c cell cycles have elapsed. Fig. 4(a) and (b) shows the cell cycle length and the age as a function of the cycle number respectively. The variable N_c is discrete and therefore Eqs. (7) and (8), instead of a curve, correspond a discrete set of values. The circles indicate precisely those values.

As mentioned above, the information obtained from the graphs of Fig. 4 is essential to our calculations as it not only determines the time integration for Eq. (2) but also provides an equivalence between elapsed number of cell cycles N_c and development time. According to the results, 38 cell cycles elapse along the entire retinogenesis and the cell cycle length varies from a little more than two hours, at early retinal development, up to about 30 h, when the birth occurs, keeping this value at postnatal stage.

Another feature observed in rat retinogenesis is that there are two phases connected by an intermediate stage (Rapaport et al., 2004). We assume then that the critical value of x, x^* which regulates the differentiation, takes two different values for each phase: a low value x_L^* for early stage and an higher value x_H^* for the late phase. The evolution between these two values is linear with cell cycle number and it occurs at intermediate stage. That is

$$x^*(N_c) = \begin{cases} x_L^* & \text{if } 1 \le N_c \le N_L, \\ \dfrac{(x_H^* - x_L^*)}{(N_H - N_L - 1)}(N_c - N_L) + x_L^* & \text{if } N_L < N_c < N_H, \\ x_H^* & \text{if } N_H \le N_c \le 38. \end{cases} \quad (9)$$

A further assumption that we will do is that the production rate of x in Eq. (2) $\beta(N_c)$ is, at first, constant and then grows linearly with the cell cycle number

$$\beta(N_c) = \begin{cases} \beta_o & \text{if } 1 \le N_c \le N^*, \\ \alpha(N_c - N^*) + \beta_o & \text{if } N^* < N_c < 38. \end{cases} \quad (10)$$

4. Retinal cell genesis

In this section we show the results obtained from our model to rat retinal development in global terms. That is, we first determine the parameters $x_L^*, x_H^*, k, v, \alpha, \beta_o, N_L, N_H$ and N^* to reproduce the experimental data of the cumulative percentage of differentiated cells as a function of development time (taken from Fig. 3 of Rapaport et al., 2004).

Then, we use these parameters to calculate other quantities of interest as a function of days of development, such as progenitor cell fraction P (and its complementary quantity Q, fraction of differentiated cells), the probability of symmetrical cell divisions leading to two progenitor cells $\Pi_{s,s}$ or two differentiated cells $\Pi_{q,q}$ and the probability of asymmetric divisions, that is producing a progenitor cell and a differentiated cell $\Pi_{q,s}$.

4.1. Determination of the parameters

As mentioned above, we first apply the model to reproduce the experimental results on the fraction of the total differentiated cells present at the end of development. Fig. 5 shows the results. The parameter values for the calculations are shown in Table 1. They are quite similar to those that describe rat neocortex development (Barton et al., 2014).

4.2. Model results

With these parameters we calculate the percentage of differentiated cells with respect to the present cells, Q and its complement P along the development. These results are depicted in Fig. 6a.

The two phases of retinogenesis can be clearly seen. They correspond to the increasing behavior of Q. Between them, there is a period in which the production of proliferative cells increases.

The probabilities for the occurrence of different kinds of divisions are shown in Fig. 6b.

Also it can be distinguished the two phases of retinogenesis. Between them there is a time period during which terminal divisions, giving two differentiated cells, are very unlikely. These

Table 1
Parameters used in the calculations.

x_L^*	x_H^*	β_o (1/day)	α (1/day)	ν (1/day)	k	N_L	N_H	N^*
1.0922	1.4494	2.2016	$3.3543\ 10^{-2}$	3.445	0.771	20	30	25

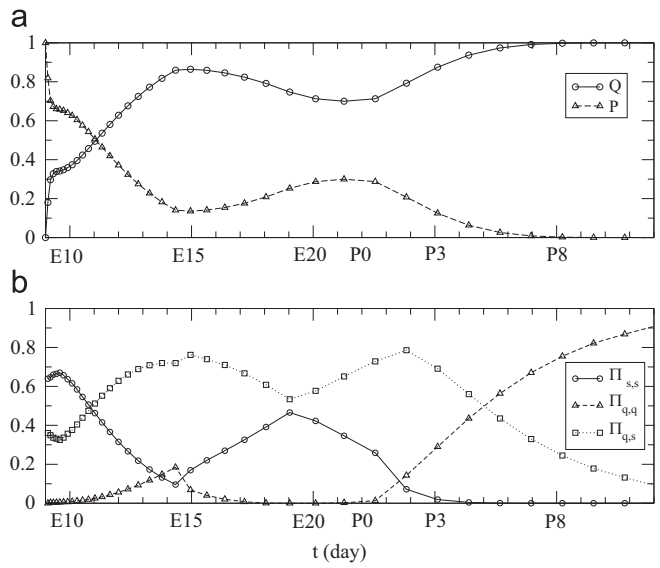

Fig. 6. (a) The fraction of differentiated (stem) cells with respect to the present cells Q (P) vs. age. (b) Probability of symmetric division giving two stem cells $\Pi_{s,s}$ (circles), symmetric division giving two differentiated cells $\Pi_{q,q}$ (triangles) and asymmetric division giving a stem cell and a differentiated cell $\Pi_{q,s}$ (squares) vs. age.

results point in the direction of the comments and discussion of Rapaport et al. (2004) regarding the early and late phases of retinogenesis.

5. Introduction of the competency

As mentioned before, during retinogenesis seven types of differentiated cells are produced. Six of them are neurons (retinal ganglion cells (G), rod (Rph) and cone (Cph) photoreceptor cells, horizontal cells (H), amacrine cells (A) and bipolar cells (B)) and one type of glia (Müller glial cells (M)). While the process of differentiation of each class of these cells is not neatly separated in time, there is a temporal order in which diverse subsets of cell types are differentiating.

It has further been determined that there is some time sequence for the beginning of the differentiation of each cell type. This gave rise to the competency model for retinogenesis (Cepko et al., 1996; Napier and Link, 2010; Gomes and Cayouette, 2010). This model proposes that the retinal neuroepithelia evolves between different states during neurogenesis so the progenitor cells are competent to generate only a subset of retinal cell types.

A simple way to introduce competency in our model is to assume that the concentration of x not only regulates the differentiation but also determines the cellular phenotype. The multiple regulation due to a single factor might seem a bit stilted. However, it has recently been found that mNumb not only could determine cell differentiation (Shimojo et al., 2011; Barton and Fendrik, 2013) but also, in retinogenesis, regulates the production of terminal asymmetric divisions (Kechad et al., 2012).

We assume that the chronological order in which differentiation for each cell type begins is the one determined for rat (Rapaport et al., 2004; Bassett and Wallace, 2012) and it is conserved in other species (LaVail et al., 1991; Harman and Beazley, 1989). That is, the sequence is G, H, Cph, A, Rph, B, M. This sequence is not strictly conserved in all species. For example in the *Xenopus leavis* there is an inversion between A and Rph (Wong and Rapaport, 2009).

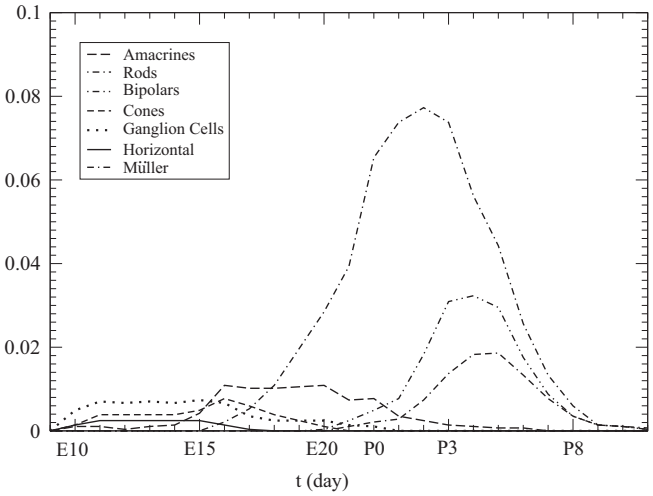

Fig. 7. Densities of production for the seven different cell types during retinogenesis vs. age, according to experimental results of Rapaport et al. (2004).

Now we define each competency state as a window on the concentration of x. We introduce six parameters, $x_G < x_H < x_{Cph} < x_A < x_{Rph} < x_B$, all greater than x_L^*. Suppose that after cell division, the concentration x in one of the daughter cells is $x > x^*(N_c)$ then, if

$x < x_G \longrightarrow$ ganglion cell,

$x_G \le x < x_H \longrightarrow$ horizontal cell,

$x_H \le x < x_{Cph} \longrightarrow$ cone photoreceptor cell,

$x_{Cph} \le x < x_A \longrightarrow$ amacrine cell,

$x_A \le x < x_{Rph} \longrightarrow$ rod photoreceptor cell,

$x_{Rph} \le x < x_B \longrightarrow$ bipolar cell,

$x_B \le x \longrightarrow$ M*üller* glia cell.

The above parameters are determined by adjusting the total percentages of each cell type when retinal development is complete. Fig. 7 reproduces the experimental data from Fig. 7 of Rapaport et al. (2004). To obtain densities, we normalize the curves dividing by the total number of cells present at the end of the development. For example, the curve corresponding to rod cells represents the fraction of the rod cells with respect to the total cells, differentiated between t and $t+dt$ and so on for all curves. Thus the total area under each curve is the fraction of each cell type at the end of development.

From these experimental data we find that a 5.7% of cells are G, 1.5% are H, 3.9% are Cph, 8.9% are A, 54.8% are Rph, 16% are B and 9.2% are M. Table 2 shows the value of the six parameters that reproduce these global values of production for each cell type. Fig. 8 shows the windows of competency and the time evolution of the critical value x^*.

For the densities predicted by our model we must consider that these give us the percentage of differentiated cells of each type in each cell cycle (not per day). To compare these densities with those depicted in Fig. 7 we must change from variable N_c to the variable t. Let $F(N_c)$ one of the densities as a function of N_c. Then, we obtain the desirable density as a function of t, $G(t)$ as

$$G(t) = F(N_c(t))\left|\frac{\delta(N_c)}{\delta t}\right|; \tag{11}$$

Table 2
Parameters that define the competency.

x_G	x_H	x_{Cph}	x_A	x_{Rph}	x_B
1.1859	1.2136	1.2913	1.4377	1.6321	1.7387

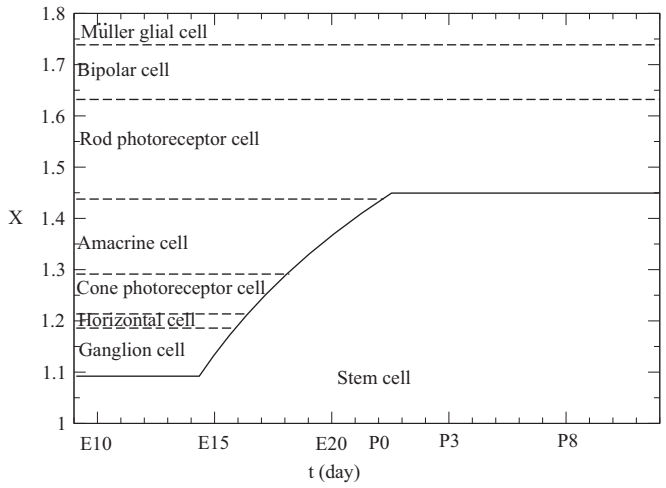

Fig. 8. Concentration of x-age domain and the critical values that define the competency states (dashed lines). The solid curve shows the evolution of the critical value x^* that regulates the cellular differentiation.

where $N_c(t)$ is given in Fig. 4b. On the other hand

$$\left|\frac{\delta(N_c)}{\delta t}\right| \sim \frac{1}{T_{N_c}}; \tag{12}$$

where T_{N_c} is given in Fig. 4a. Hence, the density as a function of t is

$$G(t) = \frac{F(N_c(t))}{T_{N_c}}. \tag{13}$$

Fig. 9 shows the seven densities corresponding to the seven cell types predicted by the model. When they are compared with the experimental densities (Fig. 7), the results are quite satisfactory. The model parameters were adjusted to reproduce global properties of retinogenesis, as the total production of differentiated cells (without discriminating phenotypes) or the total percentage of each type of cells at the end of development. On the other hand, the densities of production for each cell type differ greatly from each other and vary greatly during the development. Yet, the model results adequately describe some qualitative properties of retinogenesis identified by Rapaport et al. (2004):

1. The two phases of retinogenesis are clearly distinguished.
2. The cell production during the second phase is much greater than during the first.
3. The production of amacrine cells is related to an intermediate regime between the two phases.

The most evident difference between the experimental results and those obtained here is that the model predicts a shorter phase 1, i.e. the theoretical densities for ganglion cells, cones photoreceptor cells and amacrine cells are located more towards early days of development. In particular, unlike that reported experimentally, day after birth, practically amacrine cells are not produced while the productions of ganglion cells and cone photoreceptor cells cease quite before those that shows Fig. 7. Perhaps these discrepancies could be diminished if the model includes other sources of stochasticity that we have not taken into account, such as fluctuations in the cell cycle length.

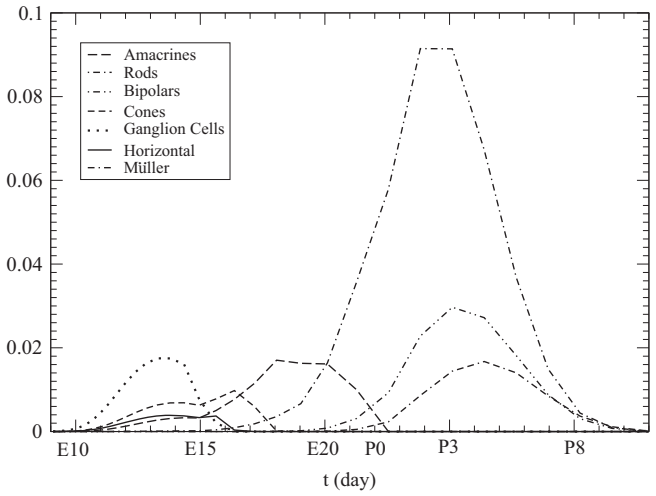

Fig. 9. The densities of production of the seven different cell types during retinogenesis vs. age, predicted by the present theoretical model.

6. Discussion and conclusions

In this work we have modeled rat retinogenesis assuming that it is a process governed by a single factor. The temporal evolution of the concentration of the factor in each cell depends on a simple dynamic equation (synthesis + degradation) during the cell cycle and a stochastic inheritance after each successive mitosis. Despite its simplicity, it is able to fairly reproduce the experimental results obtained by Rapaport et al. (2004) for complete retinogenesis. Our work attempts to explain the broader aspects of rat retinal histogenesis, taking as its starting point, the data corresponding to whole development process, as those obtained by Rapaport et al. (2004). In this framework, we have developed a phenomenological model; i.e. a modelling strategy that attempts to replicate experimental data without involving variables, parameters and equations that have a direct correspondence with the biological process (Van Ooyen, 2011). For the phenomenon modelled here, this strategy has not in mind the various networks of transcription factors that control the specification of each cell type (still under experimental characterization).

In the report of Rapaport et al. (2004), two phases separated by an intermediate regime are clearly observed. Our model reproduces this global aspect of the process, assuming:

1. The differentiation is produced from a threshold concentration of one factor or a combination of transcription factors (a ubiquitous property in the fate specifying process).
2. For each of the two phases of differentiation corresponds to a fixed threshold value (one lower and other upper), with a linear evolution between them during the transition regime.
3. The value of the variable that controls the differentiation is randomly raffled after each mitosis between daughter cells taking as average value, the value reached by the mother cell. During this process, the inherited factor values for each sister cell have an inhibitory effect between them, because their average is equal to the concentration of the mother cell. This link introduces asymmetric division (a phenomenon involved in this system).
4. The production rate of the key factor x is constant at first and then increases linearly with the cell cycle number.

With these premises, our model generates two waves of cell differentiation separated by a period of increasing stem cell production, as it is shown in the two increasing intervals of Q fraction in terms of age (Fig. 6(a))). This result is consistent with the two phases of retinogenesis (early and late) as discussed in Rapaport et al. (2004) and they are achieved due to the existence of two threshold values in the concentration of x (with a linear as a function of the cell cycle number between the two values.) As Rapaport et al. (2004) note, the curves of production of cells of phase 2 show greater amplitude than the corresponding to phase 1. To support this increase in the production of differentiated cells, Rapaport et al. (2004) hypothesize that the progenitor population is recovered by symmetrical division between the two phases, adapted to the demand to produce a higher proportion of retinal cells in phase 2 . In fact, our model predicts a reduction (nulls) for the probability for symmetric differentiative divisions (terminals, qq), between the two phases of retinogenesis. This prediction of the model has not experimentally verified yet but is in line with the discussion of Rapaport et al. (2004).

According to what is stated here, rat retinogenesis can be interpreted, at first approximation, as a process controlled by a key factor that is stochastically inherited whose concentration starting from a threshold value induces the differentiation.

In our model, the source of stochasticity is cell division. When it occurs, a key factor is inherited by daughter cells according to a probability distribution. Its asymmetric inheritance is the basis for the diversification of cell fates. One possible source of this is the asymmetric inheritance of Numb in late RPCs (Kechad et al., 2012) or asymmetric inheritance of fate determinants. Thus, our model considers in a unified view, the succession in competency states given by Cepko et al. (1996) and Livesey and Cepko (2001) and the role of stochasticity proposed by Gomes et al. (2011) and He et al. (2012), and it globally reproduces the entire rat retinogenesis reported by Rapaport et al. (2004).

In the introduction we have discussed recent findings that reveal the existence of specified RPCs producing specific pairs of sister cells in terminal divisions. These findings seem to contradict the role of stochasticity in developing retina. On this point, it is important to characterize the lineages of RPCs upstream of the specified RPCs to determine if there are stochastic events that generate characteristic distributions of these terminally dividing cells. If so, the distribution of the cell types of the adult retina could be the result of a sequential evolution in competency states and probabilistic events introduced by asymmetric division, as described by our model.

The present approach involves results at tissue level, without considering the detailed molecular aspects that control the process. In fact, it is known that the specification for each retinal phenotype is produced by a specific combination of bHLH and homeobox transcription factors (transcription factor code) (Ohsawa and Kageyama, 2008). However, it is unknown how the transitions between these different expression patterns occur. In light of this, one possible interpretation of the results of our model is that the different threshold values in the concentration of a key factor activate the different transcriptional networks involved in the specification of each cell type.

There is evidence to suggest the existence of a molecular link between the cell cycle length and the evolution of the competency states. For example, it has been proposed that the increase in the cell cycle length of late RPC allows a reduction in the concentration of miRNAs that regulate the translation of two transcription factors: *Otx2* and *vsx1*, allowing their translation and activating the dipolar cell fate (Decembrini et al., 2009). Such findings are interesting in light of the results obtained in our model, in which we assume the evolution of the value that determines the succession of competency states (determined by the evolution of the x) and the increase of cell cycle length along the development of the retina taken from data provided by Alexiades and Cepko (1996). Furthermore, it has been found that a set of three microRNAs (let7, microRNA-125 and microRNA-9) are key regulators in the competency transition from the early phenotypes to the late phenotypes (La Torre et al., 2013). Other studies have identified transcription factors involved in the temporal progression of cell fates. Such is the case of Ikaros, a vertebrate transcription factor homologous to Hunchback that specifies early fates in the ventral nerve cord of *Drosophila*. This transcription factor is involved in the specification of early fates in the vertebrate retina (Elliott et al., 2008).

Acknowledgment

This work was partially supported by PIP 00365/11 (CONICET—Argentina).

References

Alexiades, M.R., Cepko, C., 1996. Quantitative analysis of proliferation and cell cycle length during development of rat retina. Dev. Dyn. 205, 293–307.
Barton, A., Fendrik, A.J., 2013. Sustained vs. oscillating expression of Ngn2, Dll1 and Hes1: a model of neural differentiation of embryonic telencephalon. J. Theor. Biol. 328, 1–8.
Barton, A., Fendrik, A.J., Rotondo, E., 2014. A stochastic model of neurogenesis controlled by a single factor. J. Theor. Biol. 355, 77–82.
Bassett, E.A., Wallace, V.A., 2012. Cell fate determination in the vertebrate retina. Trends Neurosci. 35, 565–573.
Belliveau, M.J., Cepko, C.L., 1999. Extrinsic and intrinsic factors control the genesis of amacrine and cone cells in the rat retina. Development 1126, 555–566.
Belliveau, M.J., Young, T.L., Cepko, C.L., 2000. Late retinal progenitor cells show intrinsic limitations in the production of cell types and the kinetics of opsin synthesis. J. Neurosci. 20, 2247–2254.
Cayouette, M., Barres, B.A., Raff, M., 2003. Importance of intrinsic mechanisms in cell fate decisions in the developing rat retina. Neuron 40, 897–904.
Cayouette, M., Poggi, L., Harris, W.A., 2006. Lineage in the vertebrate retina. Trends Neurosci. 29, 563–570.
Cayouette, M., Raff, M., 2003. The orientation of cell division influences cell-fate choice in the developing mammalian retina. Development 130, 2329–2339.
Cepko, C.L., Austin, C.P., Yang, X., Alexiades, M., Ezzeddine, D., 1996. Cell fate determination in the vertebrate retina. proc. Natl. Acad. Sci. USA 93, 589–595.
Cepko, C., 2014. Intrinsically different retinal progenitor cells produce specific types of progeny. Nat. Rev. Neur. 15, 615–627.
Collins, R.T., Linker, C., Lewis, J., 2010. MAZe: a tool for mosaic analysis of gene function in zebrafish. Nat. Methods 7, 219–223.
Decembrini, S., Bressani, D., Vignali, R., Pitto, L., Mariotti, S., Rainaldi, G., Wang, X., Evangelista, M., Barsacchi, G., Cremisi, F.D., 2009. MicroRNAs couple cell fate and developmental timing in retina. Proc. Natl. Acad. Sci. USA 106, 21179–21184.
Elliott, J., Jolicoeur, C., Ramamurthy, V., Cayouette, M., 2008. Ikaros confers early temporal competence to mouse retinal progenitor cells. Neuron 60, 26–39.
Gomes, F.L.A.F., Zhang, G., Carbonell, F., Correa, J.A., Harris, W.A., Simons, B.D., Cayouette, M., 2011. Reconstruction of rat retinal progenitor cell lineages in vitro reveals a surprising degree of stochasticity in cell fate. Dev. Stem Cells 138, 227–235.
Gomes, F.L.A.F., Cayouette, M., 2010. Retinal development: cell type specification. In: Lemke, G. (Ed.), Developmental Neurobiology. Academic Press, Elsevier, London, Burlington, San Diego, pp. 259–270.
He, J., Zhang, G., Almeida, A.D., Cayouette, M., Simons, B.D., Harris, W.A., 2012. How variable clones build an invariant retina. Neuron 75, 786–798.
Harman, A.M., Beazley, L.D., 1989. Generation of retinal cells in the wallaby, *Setonix brachyurus* (quokka). Neuroscience 28, 219–232.
Jusuf, P.R., Almeida, A.D., Randlett, O., Joubin, K., Poggi, L., Harris, W.A., 2011. Origin and determination of inhibitory cell lineages in the vertebrate retina. J. Neurosci. 31, 2549–2562.
Kechad, A., Jolicoeur, C., Tufford, A., Mattar, P., Chow, R.W.Y., Harris, W.H., Cayouette, M.R., 2012. Numb is required for the production of terminal asymmetric cell divisions in the developing mouse retina. J. Neurosci. 32, 17197–17210.
Klein, A.M., Simons, B.D., 2011. Universal patterns of stem cell fate in cycling adult tissues. Development 138, 3103–3111.
La Torre, A., Georgi, S., Reh, T.A., 2013. Conserved microRNA pathway regulates developmental timing of retinal neurogenesis. Proc. Natl. Acad. Sci. 110, E2362–2370.
LaVail, M.M., Rapaport, D.H., Rakic, P., 1991. Cytogenesis in the monkey retina. J. Comp. Neurol. 309, 86–144.
Li, X., Chen, Z., Desplan, C., 2013. Temporal patterning of neural progenitor in *Drosophila*. Curr. Top. Dev. Biol. 105, 69–96.
Livesey, F.J.A., Cepko, C.L., 2001. Vertebrate neural cell-fate determination: lessons from the retina. Nat. Rev. Neurosci. 2, 109–118.
Napier, H.R.L., Link, B.A., 2010. Retinal development: an overview. In: Lemke, G. (Ed.), Developmental Neurobiology. Academic Press-Elsevier, London, Burligton, San Diego, pp. 251–258.

Ohsawa, R., Kageyama, R., 2008. Regulation of retinal cell fate specification by multiple transcription factors. Brain Res. 1192, 90–98.
Rapaport, D.H., Wong, L.L., Wood, E.D., Yasumura, D., LaVail, M.M., 2004. Timing and topography of cell genesis in the rat retina. J. Comp. Neurol. 474, 304–324.
Shimojo, H., Ohtsuka, T., Kageyama, R., 2011. Dynamic expression of Notch signaling genes in neural stem progenitor cells. Front. Neurosci. 5, 1–7.
Slater, J.L., Landman, K.A., Hughes, B.D., Shen, Q., Temple, S., 2009. Cell lineage tree models of neurogenesis. J. Theor. Biol. 256, 164–179.
Trimarchi, J.M., Stadler, M.B., Cepko, C.L., 2008. Individual retinal progenitor cells display extensive heterogeneity of gene expression. PLoS ONE 3, e1588.
Turner, D.L., Cepko, C.L., 1987. A common progenitor for neurons and glia in rat retina persists in late development. Nature 328, 131–136.
Turner, D.L., Snyder, E.Y., Cepko, C.L., 1999. Lineage-independent determination of cell type in the embryonic mouse retina. Neuron 4, 833–845.
Van Ooyen, A., 2011. Using theoretical models to analyse neural development. Nsat. Rev. Neurosci. 12, 311–326.
Wong, L.L., Rapaport, D.H., 2009. Defining retinal progenitors cell competence in *Xenopus leavis* by clonal analysis. Development 136, 1707–1715.